NEW FRONT. CHEM. (2020)
Volume 29, Number 2, pp. 69-97
ISSN 2668-9189; ISSN-L 2393-2171

Former: Ann. West Univ. Timisoara – Series Chem.
ISSN: 1224-9513

Article

TOPO-CHEMICAL REACTIVITY STUDY ON MOLECULAR MACHINES

Nicoleta A. Dudaş[1], Ottorino Ori[1,2], and Mihai V. Putz [1,3](♣)

(1) Laboratory of Structural and Computational Physical-Chemistry for Nanosciences and QSAR, Biology-Chemistry Department, West University of Timisoara, Pestalozzi Street No. 16, Timisoara, RO-300115, Romania

(2) Actinium Chemical Research, Via Casilina 1626/A, 00133 Rome, Italy

(3) Laboratory of Renewable Energies-Photovoltaics, R&D National Institute for Electrochemistry and Condensed Matter, Dr. A. Paunescu Podeanu Str. No. 144, Timisoara, RO-300569, Romania

ABSTRACT

A topological-chemical reactivity studies (using electronegativity, chemical hardness, chemical power, electrophilicity indices and topological indices like Wiener indice) has been applied on calixare-based rotaxane complexes containing tris(N-phenylureido)-calix[6]arene as wheel and a 4,4'-bipyridinium dication's units as axle. The results indicate that the formation of this type of rotaxanic complex needs a preorganisational modifications undertaken by the calixarene to match with its molecular surface the shape of the guest molecule (axle of rotaxane). The obtained chemical binding scenario suggests that we are dealing with a system that remains open until the delayed maximization of the HOMO-LUMO interval, fact that allows the continuous transfer of charge between the components of the rotaxane.

Keywords: Molecular mashines, Rotaxane; Calixarene; Chemical reactivity indices, Wiener indices.

1. INTRODUCTION

Supramolecular chemistry, "the chemistry beyond the molecule" [1-3] is one of the trends of the last decades; a domain that continues to grow in many directions/fields and won two Nobel prize in the last 30 years [1-3]. Nowadays supramolecular chemistry is a highly interdisciplinary field and is composed of many expanding areas with many different

♣ Correspondent author: Tel: +40-256-592638, Fax: +40-256-592620; E- mails: mv_putz@yahoo.com or mihai.putz@e-uvt.ro

applications. From this point of view we can mention: mechanically interlocked molecules (MIMs), molecular machines and motors, molecular sensors (chemosensors), etc. [1-10]. In the case of these assemblies like mechanically interlocked molecules, the molecules are not chemically bonded; the molecules interact through intermolecular bonds and/or forces and come together resulting complexes with new and better properties [1-10]. A new concept introduce in the last years in supramolecular interactions is the *mechanical bond* which is the driving force for mechanically interlocked molecules (MIMs) [3,4].

Molecules that are connected as a consequence of their topology are named *Mechanically interlocked molecular architectures*; these interlocked molecules cannot be separated without the breaking of the covalent bonds that comprise the conjoined molecules. [4,10-12]. As mechanically interlocked molecular architecture are known rotaxanes and catenanes. Rotaxanes are composed of one or more axles/threads (the dumbbell components) which is surrounded by one or more rings/wheel (an macrocyclic compound) while catenanes are made of (at least) two interlocked macrocycles (rings) [4,10,13-16]. (see Figure 1). These compounds have many application in different field like chemistry, biology, medicine and in materials research, they can be used as drug delivery agents, catalysts, in molecular electronics as logic molecular switching elements, as molecular shuttles etc [4,10,15-21].

Figure 1: Schematic structures of molecular machines: *left* – rotaxanes structures, *right* – catenanes structures

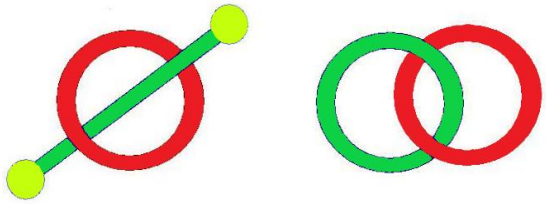

The rotaxanes axle is terminated by bulky end-groups (stoppers) that prevent that these complexes to disassembly [4,10,13-16]. If the bulky groups are too small or they do not exist, the complexes are named as pseudorotaxanes [4,10,14]. The rotaxane ring can made two molecular motions: *rotation motions* – it is rotating around the axis of the dumbbell; or *translation motions* – it is sliding along its axle from one site to another [4,10,13-16].

One of the chemical species that are used to made the dumbbell component of the rotaxanes are bipyridine unit (a dicationic viologen axle) to which are attached alkyl chains of different lengths (symmetrical or not) which may have various bulky end-groups (stoppers) [10,16,22-27]. These 4,4'-bipyridinium dications are an electron accepting units, an electron-poor π-systems that exhibit quite different physico-chemical properties (as evidenced by photophysical, photochemical and electrochemical investigations, quantum chemical calculations [10,16,25-27]) and are widely used in the construction of molecular devices [10,16,22-27] (see Figures **2** and **3**).

Calixarenes are now very popular building blocks in many diverse areas as molecular and supramolecular systems like rotaxanes, but also they are used in the synthesis of nanoparticles-based architectures and catalysis, for their biological applications, etc. [10,16,21,28-34]. All these applications of calixarenes are due to their properties like: high chemical and thermal

stability, high melting points, low solubility and toxicity, their synthetic availability and the presence of reactive sides, structures that can relatively be easily modified [10,16,21,28-34].

Figure 2: *Left* - the 4,4'-bipyridinium dication unit - axle in rotaxane complex; *Right* - tris(N-phenylureido)-calix[6]arene - the calixarene wheel in rotaxane complex

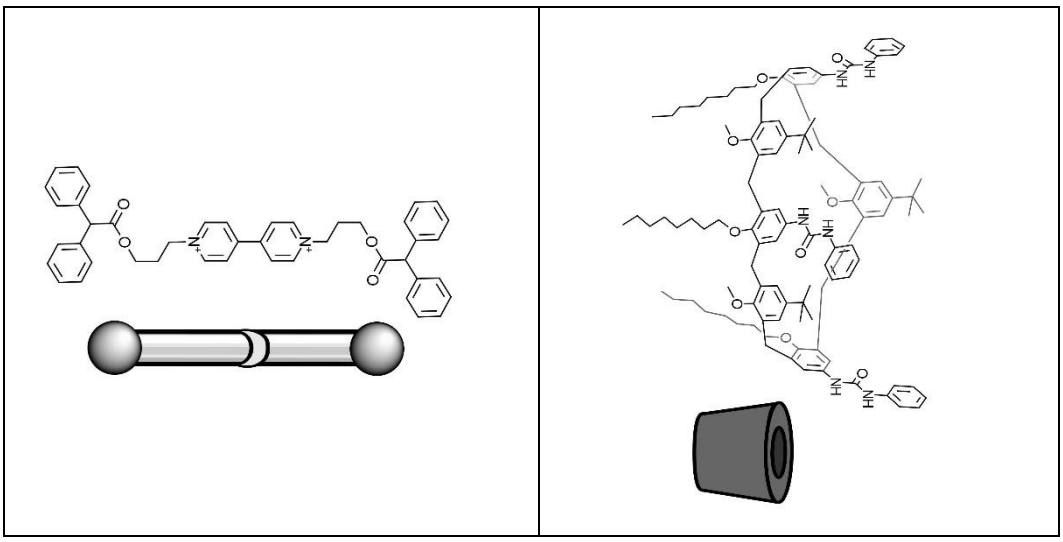

Figure 3 Calixarene-based rotaxane **1_4** which contain as wheel tris(N-phenylureido)-calix[6]arene and as axle a 4,4'-bipyridinium dication unit

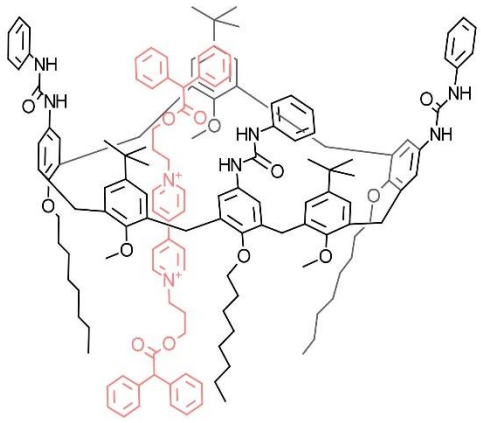

Molecular machine complexes like **1_4, 2_4 or 3_4** (see Figure **3** and **4**) are rotaxane -type systems wich contain calyx[6]arene wheel like tris(N-phenylureido)-calix[6]arene (compound **4**) and bipyridinium units as axle (compounds **1, 2, 3**), have been extensively researched in the last decades[10,16,22-27,35-44]. For the dicationic rotaxanes like **1_4, 2_4 or 3_4,** the counteranions can be tosylate, iodine, etc [10,16,22-27]. These complexes are stabilized together through solvophobic effects and several non-covalent interactions like: hydrogen bonds, CH-π and charge-transfer interactions between the π-electron poor bipyridinium unit

and the π-electron rich cavity of the wheel [10,16,22,23,38]. NH-moiety from ureidic groups located on the upper rim of the wheel can make hydrogen bonds with the counteranions (e.g.: tosylate) fact that will lead to the stabilization of the complex [10,16,22,23,38]. It seems that the solvent do not affect the behavior of the central 4,4'-bipyridinium unit in the case of the complex **1_4** (see Figure **3)** [10,16,22,23,39]**.**. This complex have the shortest 4,4'-bipyridinium axle wich is deeply encapsulated within the wheel–stoppers ensemble [10,16,22,23,39]. In rotaxanes (or catenanes) molecular mashines based on calix[6]arene, the wheel of rotaxane complex can present many geometries, different conformations: cone, a partial cone, [(1,2), (1,3), (1,4)]-alternate, [(1,2,3), (1,2,4), (1,3,5)]-alternate,. This geometries/conformation of the calix[6]arene depend on the type and number of the substituents situated on upper or lower rim [22-27,31,35-46] and have been very intense investigated in the last years (the synthesis, co-conformational switching, atropoisomerism, their properties (e.g. redox properties), etc.) [22-27,31,40-46].

Figure 4: Structures of the three 4,4'-bipyridinium dication unit - axle in rotaxane complex (**1, 2, 3**) and the tris(N-phenylureido)-calix[6]arene (**4**) - the calixarene wheel in rotaxane complex

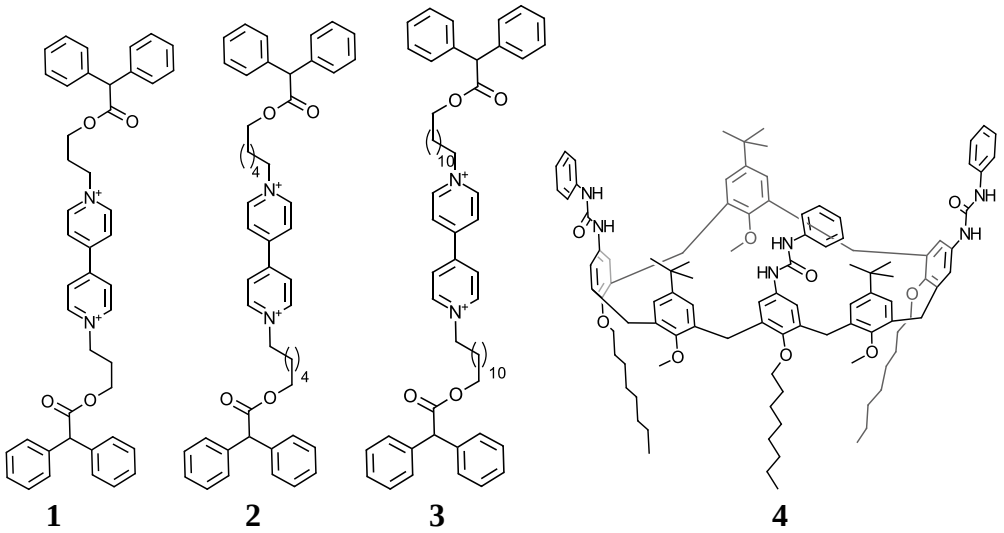

So far, in the literature can be found studies that reveal the mechanism of chemical-biological interaction between the biological receptor and the chemical ligand using the chemical reactivity indicators [10,47,48] and topological relation between chemical structure and biological activity [49]. Referring to calixarenes, rotaxane and molecular machines it seems that are missing topological-chemical reactivity studies (such as those who are using electronegativity, chemical hardness, chemical power, electrophilicity indices and topological indices like Wiener indice).

2. METHOD

2.1. Theoretical Model

The molecular orbitals HOMO and LUMO, provides basic chemical reactivity indices. The molecular structure include the key pathway to chemical reactivity through their HOMO and LUMO. This chemical reactivity indices combine with their associated chemical principles can be interpreted in QSAR models and not only [10,47,48,50]. This basic chemical reactivity indices are electronegativity (χ), chemical hardness (η), chemical power index (π), electrophilicity (ω) which are defined:

- electronegativity (χ) is negative of the chemical potential [10,47,51-54], through the derivation of the total energy with respect of the total number of electrons, reducing in the finite/central difference approximation to the celebrated Mulliken formula [10,47,55]:

$$\chi \equiv -\mu \equiv -\left(\frac{\partial E_N}{\partial N}\right)_{V(\mathrm{r})} \cong -\frac{E_{LUMO}+E_{HOMO}}{2} \qquad (1)$$

- chemical hardness (η) is the negative variation of electronegativity with respect of the total electrons in the system [10,47,56-59], also approximates in the finite difference with HOMO–LUMO information simply as [10,47,60]:

$$\eta = -\chi \equiv -\frac{1}{2}\left(\frac{\partial \chi}{\partial N}\right)_{V(\mathrm{r})} \equiv \left(\frac{\partial^2 E_N}{\partial N^2}\right)_{V(\mathrm{r})} \cong \frac{E_{LUMO}-E_{HOMO}}{2} \qquad (2)$$

- chemical power index (π) is the half ratio of electronegativity-to-chemical hardness that models the electronic charges exchanged through the adducts in minimizing the resulting bonded complex electronegativity [10,47,50]:

$$\pi = \frac{\lambda}{2\eta} = \frac{1}{2}\frac{\chi_A}{\eta_B} = \frac{1}{2}\tan(\theta_A) \cong -\Delta N_A \qquad (3)$$

- electrophilicity (ω) is the coupling of chemical power index with electronegativity to provide the energetic information of activation towards charge tunneling of the potential barrier between adducts [10,47]:

$$\omega = \chi \times \pi = \frac{\chi^2}{2\eta} \qquad (4)$$

Chemical principles of this chemical reactivity indices are [10,47,48]:

- Minimum electronegativity principle eqs. (5)
- Maximum hardness principle eqs. (6)
- Minimum chemical power index principle eqs. (7)
- Minimum electrophilicity principle (double minimum character) eqs. (8)

$$\delta\chi \le 0 \qquad (5)$$
$$\delta\eta \ge 0 \qquad (6)$$
$$\delta\pi \le 0 \qquad (7)$$

$$\delta\omega \leq 0 \tag{8}$$

The hierarchy for chemical binding scenario [10,61] is leaving with the conducted hierarchy eqs. (9) [10,47,48,61,62]:

$$\chi \rightarrow \eta \rightarrow \pi \rightarrow \omega \tag{9}$$

Namely a chemical reaction/interaction is triggered by electronegativity (its difference) and its minimizing principle, followed by chemical hardness maximization of the interacting frontier orbitals implying maximum energy in charge exchange (parallel spins) followed by minimum activation by adducts' potential barrier tunneling (spin pairing) [10,47,48,61,62]. However, when is about a chemical interaction through non-covalent bonding and/or mechanical bonding, such chemical hierarchy is may lead with various hierarchical configurations [10,47,48].

Topological indices like *Wiener index W* have been successfully applied to emphasize *the stability of the chemical structure* [49,63-66]. The *Wiener index W* of the whole chemical graph G is the sum of the *Wiener-weights* w_v [49,63-66]:

$$W = \sum_{v=1}^{N} w_v \tag{10}$$

In the chemical graph G with N nodes and B bonds, the *chemical distance* d_{vu} is merely the number of bonds connecting, along the shortest path, any pairs of atoms in the system, namely the two nodes *v* and *u*, with d_{vv}=0 by definition [49,63-66]. With the name *Wiener-weight* w_v of the node *v* we call the the half-summation of the minimum distances d_{uv} between all pairs of G(N) vertices, meaning the invariant [49,63-66]:

$$w_v = \frac{1}{2}\sum_{u=1}^{N} d_{uv}, d_{vv} = 0, u, v = 1,2,\ldots, N \tag{11}$$

The *Wiener-weight* w_v it is inversely proportional to the *reactivity* of the node and to the *compactness* of the graph. *The Wiener index W* of the whole graph is just the sum of the Wiener-weights eqs. (10) [49,63-66]. Also the *Wiener-weight* w_v allows the direct topological measure of the topological roundness of the graph: *the topological efficiency index* ρ and the *extreme topological efficiency index* ρ^E [49,63-66]:

$$\rho = WN / \underline{w} \tag{12}$$

$$\rho^E = \overline{w} / \underline{w} \tag{13}$$

in which $\underline{w}$ = min{ w_v } and $\overline{w}$ = max{ w_v }.

It is noticeable that the most compactly-embedde vertices of G (the so-called *minimal vertices or minimal nodes*) have Wiener-weight w_v equal to $\underline{W}$ and also that *the smallest is the topological efficiency index, the highest is the stability of the chemical structure under examination* eqs. (14), eqs. (15) [49,63-66].

$$\rho \geq 1 \tag{14}$$

$$\rho^E \geq 1 \tag{15}$$

Table 1. Total energy and the parameters of chemical reactivity calculated for rotaxanes **1_4, 2_4, 3_4** under study, which are in the precomplex stage as well as complexes; Δ – is the differences between complex and precomplex state.

PRECOMPLEX	$HOMO_{precomplex}$	$LUMO_{precomplex}$	$\chi_{precomplex}$ (eV)	$\eta_{precomplex}$ (eV)	$\pi_{precomplex}$	$\omega_{precomplex}$ (eV)	$Etotal_{precomplex}$ (kcal/mol)
1:4	110.8641	117.7821	-114.3231	3.459	-16.52545533	1889.241283	3702346.613
2:4	82.58545	84.71627	-83.65086	1.06541	-39.25759097	3283.931247	3621720.058
3:4	-144.966	-143.0296	143.9978	0.9682	74.36366453	10708.20409	3477598.596
COMPLEX	$HOMO_{complex}$	$LUMO_{complex}$	$\chi_{complex}$ (eV)	$\eta_{complex}$ (eV)	$\pi_{complex}$	$\omega_{complex}$ (eV)	$Etotal_{complex}$ (kcal/mol)
1_4	-5.43268	-5.06872	5.2507	0.181979	14.42666	75.75009	3837167.691
2_4	32.81105	33.90942	-33.360235	0.549185	-30.37249288	1013.2335	3870660.029
3_4	-88.8077	-87.3996	88.10365	0.704085	62.56606	5512.298	4045342.867
Δ=Complex -Precomplex	$\Delta HOMO_{complex-precomplex}$	$\Delta LUMO_{complex-precomplex}$	$\Delta\chi_{complex-precomplex}$ (eV)	$\Delta\eta_{complex-precomplex}$ (eV)	$\Delta\pi_{complex-precomplex}$	$\Delta\omega_{complex-precomplex}$ (eV)	$\Delta Etotal_{complex-precomplex}$ (kcal/mol)
Case 1_4	-116.296779	-122.850821	119.5738	-3.277021	30.95211995	-1813.491195	134821.0774
Case 2_4	-49.7744	-50.80685	50.290625	-0.516225	8.885098099	-2270.697747	248939.9723
Case 3_4	56.15827	55.63004	-55.894155	-0.264115	-11.79760717	-5195.906385	567744.2707

2.2. Computational Model

For our study we choose the molecular mashine complexes **1_4, 2_4, 3_4** formed from the 4,4'-bipyridinium dication unit **1, 2 and 3** and the wheel of rotaxane made of calyx[6]arene with three N-phenylureido groups on the upper rim of the wheel **(4)** (see Figure 3 and 4) [22,23,39]**.**

We have calculated the chemical reactivity parameters (electronegativity (χ), chemical hardness (η), chemical power index (π), electrophilicity (ω)) for the two stages of the rotaxane molecular machine: precomplexes (**1:4, 2:4, 3:4)** and rotaxane molecular complexes (**1_4, 2_4, 3_4)**. The values of HOMO, LUMO orbitals energies are calculated using the semiempirical method (AM1) (Polak-Ribiere conjugate gradient algorithm and single point geometry optimization) as provided by Hyperchem 7.01 [67], while the values of chemical reactivity parameters were calculated using those for HOMO and LUMO and Eqs. (1), (2), (3), and (4) (see Table 1). For all stages (precomplex and complex) also was calculated the total energy using the same semiempirical method (AM1) and also was calculated the difference between the complex and precomplex stage. All the results are summarized in Table 1.

The molecular structures of calix[6]arenes complexes with three kinds of guest, molecular complexes **1_4, 2_4, 3_4** in the partial cone conformation have been herewith studied by ab-initio and topological methods (see Table 2). Energy calculations have been performed to gain more insight on the stabilizing effects coming by the host-guest interactions.

Table 2. *Wiener index W, the topological efficiency index ρ* and the *extreme topological efficiency index* ρ^E for the complexes in work

Rotaxane complex	W	ρ	ρ^e	W_{exp}
1_4	13719	1.322313	1.703614	*35.92726*
2_4	20786	1.32092	1.701068	*39.41446*
3_4	40968	1.324111	1.716484	*46.39794*

3. RESULTS AND DISCUSSIONS

We performed the correlation between the total energy, the chemical reactivity indices and the Wiener indices for the rotaxane molecular complexes (**1_4, 2_4, 3_4),** and for the Δ-stage (the difference between the complex and precomplex stage), the results being included in Table 3.

Table 3: Correlation between the energy, the chemical reactivity indices and the Wiener indices for the rotaxane molecular complexes (**1_4, 2_4, 3_4),** and also for the Δ-stage (the difference between the complex and precomplex stage)

The linear regression equation and the graph of the obtained equation, R and R^2 values	**The linear regression equation and the graph of the obtained equation, R and R^2 values**
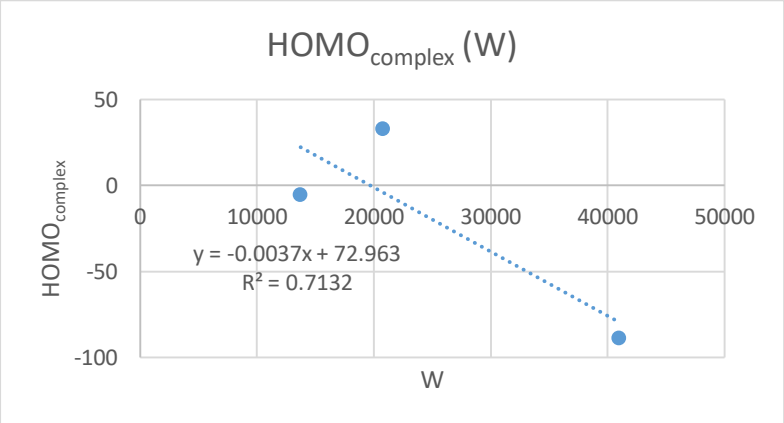 **$HOMO_{complex}(W)$ = -0.003714 W**+ 72.96345 R = 0.84453578	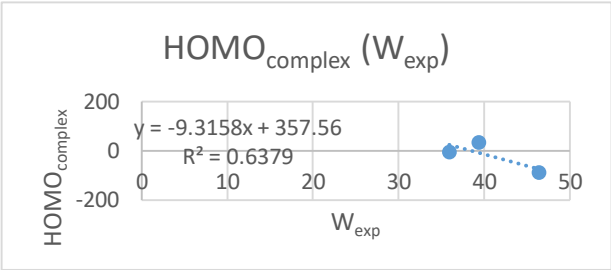 **$HOMO_{complex}(W_{exp})$ = -9.315836 W_{exp}** + 357.559148 R = 0.79868301
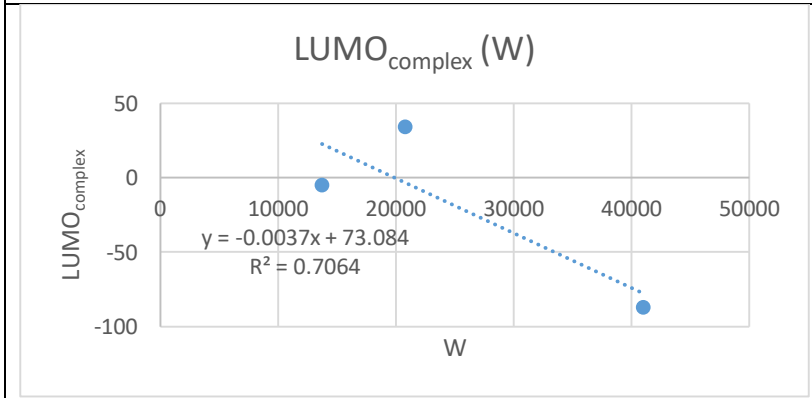 **$LUMO_{complex}(W)$ = -0.00368 W**+ 73.083705 R = 0.8327144	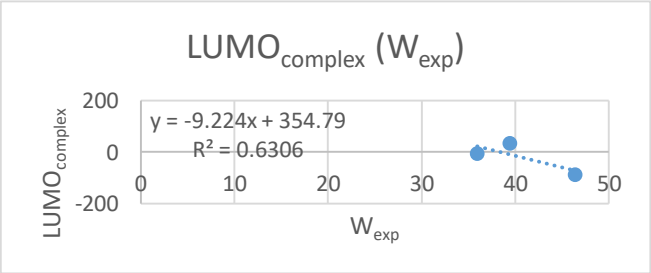 **$LUMO_{complex}$ (W_{exp}) = -** 9.22403465 **W_{exp}** + 354.790675 R = 0.79409727

The linear regression equation and the graph of the obtained equation, R and R^2 values	**The linear regression equation and the graph of the obtained equation, R and R^2 values**
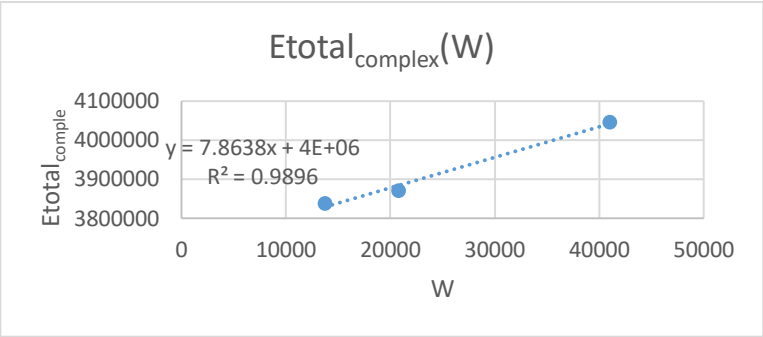 **Etotal$_{complex}$(W)** = 7.8638 **W**+ 3719888.59 R = 0.99478401	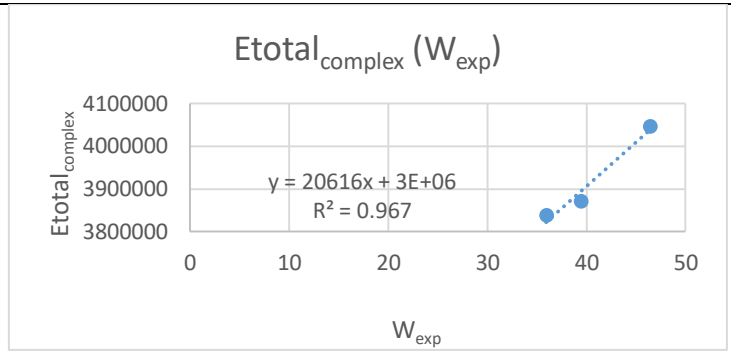 **Etotal$_{complex}$(W$_{exp}$)** = 20616.3738 **W$_{exp}$** + 3081113.38 R = 0.98334296
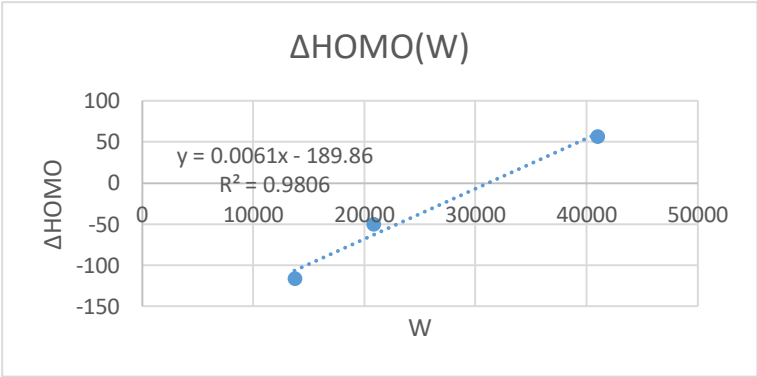 **ΔHOMO(W)** = 0.00609 **W**-189.862798 R = 0.99023547	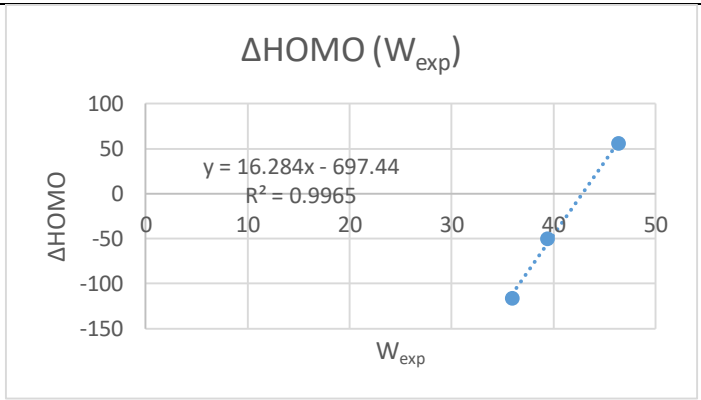 **ΔHOMO (W$_{exp}$)** = 16.284015 **W$_{exp}$** - 697.44118 R = 0.99824428

The linear regression equation and the graph of the obtained equation, R and R^2 values	The linear regression equation and the graph of the obtained equation, R and R^2 values
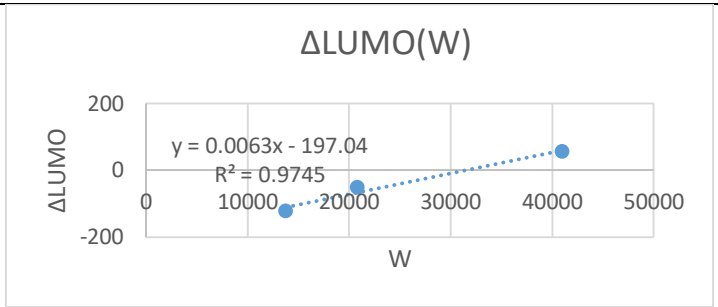 **ΔLUMO(W) = 0.**006268 **W**-197.042346 R = 0.98718854	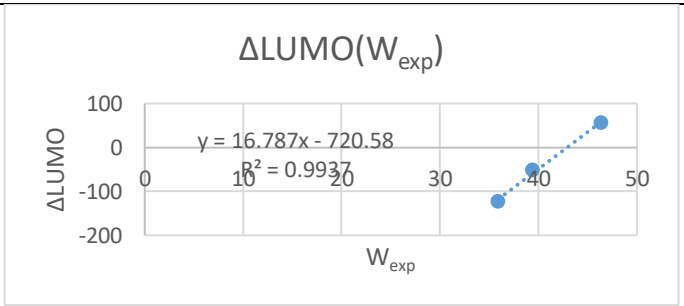 **ΔLUMO(W_{exp})** = 16.78746 **W_{exp}** - 720.57596 R = 0.99682972
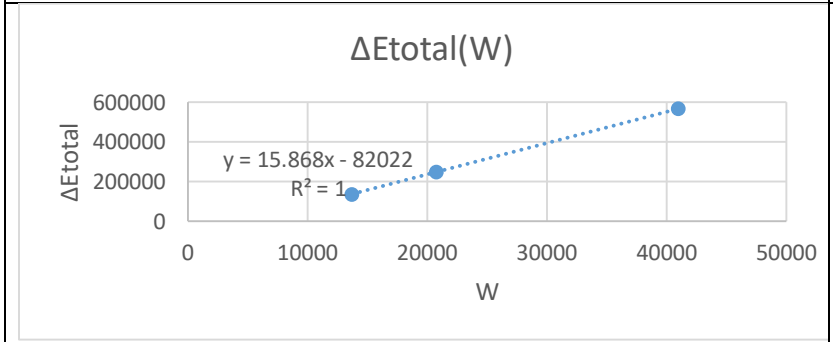 **ΔEtotal (W)** = 15.86755 **W** -82022.1259 R = 0.99998959	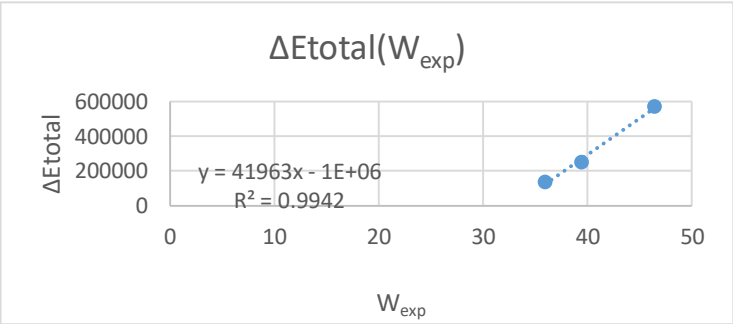 **ΔEtotal (W_{exp})** = 41962.504 **W_{exp}** -1385665.29 R = 0.99711105

The linear regression equation and the graph of the obtained equation, R and R^2 values	**The linear regression equation and the graph of the obtained equation, R and R^2 values**
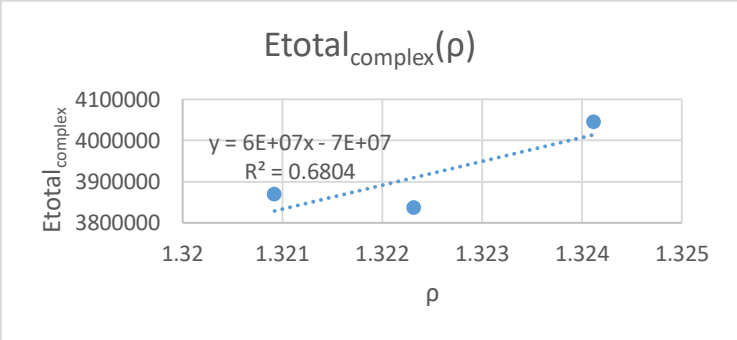 **Etotal$_{complex}$(ρ)** = 57636021.9 **ρ** -72302930.135 R = 0.82485348	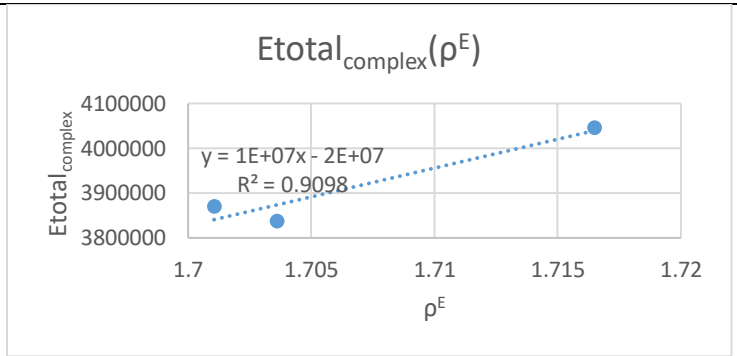 **Etotal$_{complex}$ (ρ^E)** = 12902072.77 **ρ^E** -18106826.89 R = 0.95382083
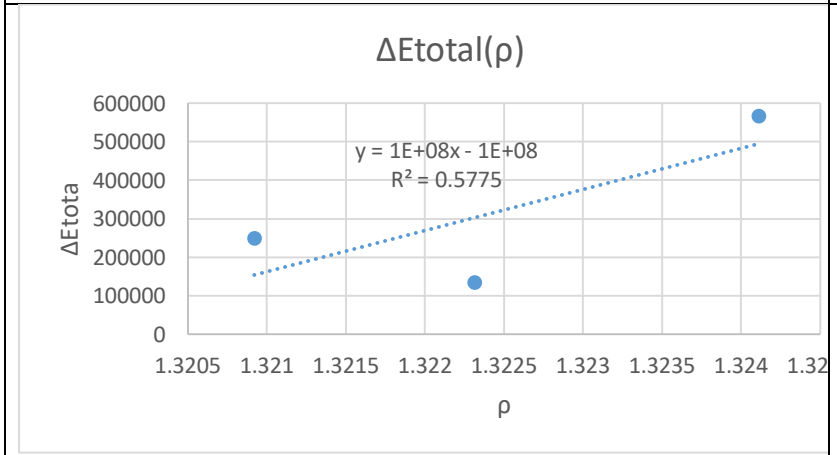 **ΔEtotal(ρ)** = 106585627.65 **ρ** -140636803.35 R = 0.75992522	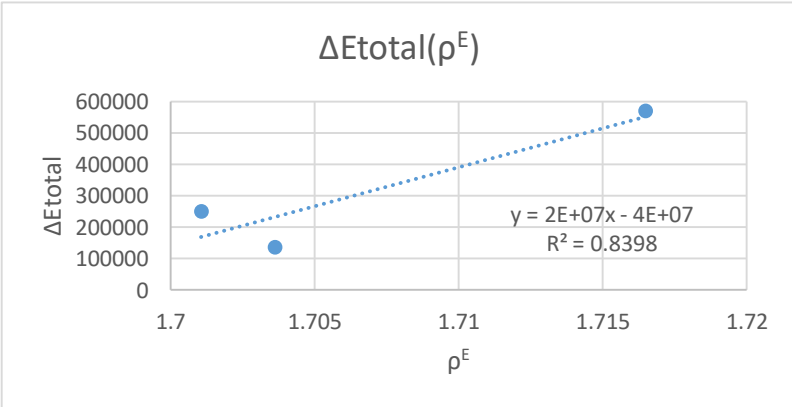 **ΔEtotal(ρ^E)** = 24881879.8 **ρ^E** - 42157573.89 R = 0.91638907

The linear regression equation and the graph of the obtained equation, R and R^2 values	The linear regression equation and the graph of the obtained equation, R and R^2 values
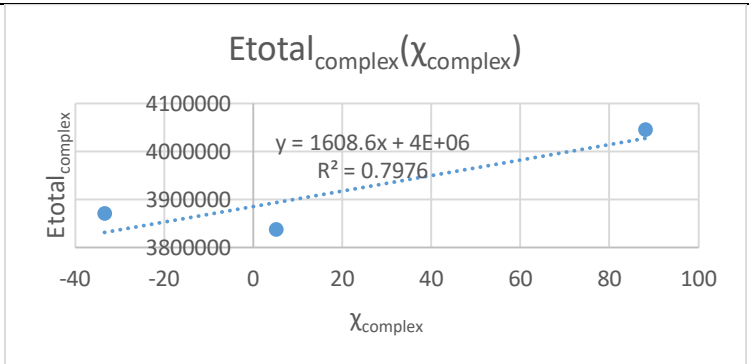 **Etotal$_{complex}$ ($\chi_{complex}$)** = 1608.57629 $\chi_{complex}$ + 3885555.16 R = 0.89305771	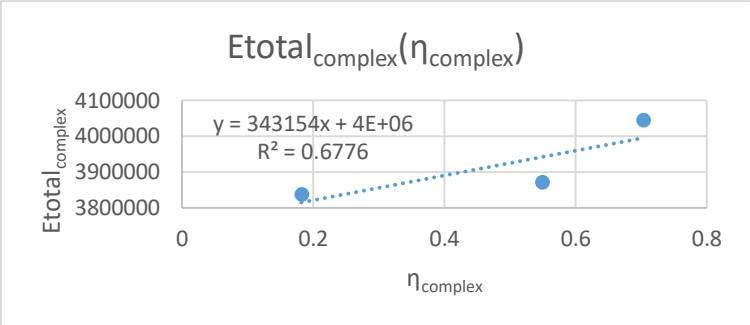 **Etotal$_{complex}$ ($\eta_{complex}$)** = 343153.77 $\eta_{complex}$ + 3753553.15 R = 0.82317418
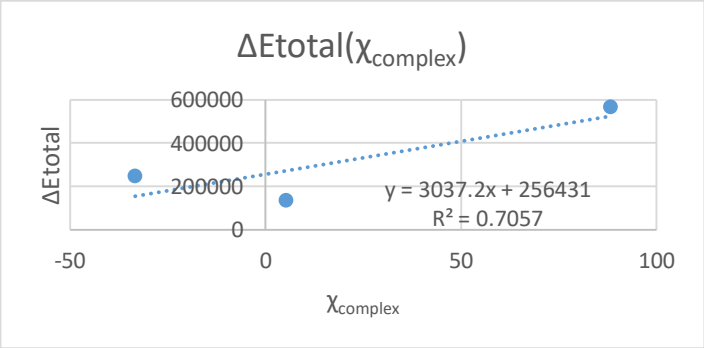 **ΔEtotal ($\chi_{complex}$)** = 3037.183289 $\chi_{complex}$ + 256430.73 R = 0.84003670	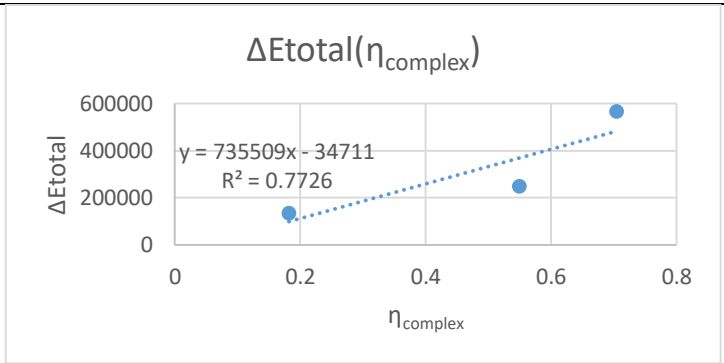 **ΔEtotal ($\eta_{complex}$)** = 735508.68 $\eta_{complex}$ - 34710.9273 R = 0.87898236

The linear regression equation and the graph of the obtained equation, R and R^2 values	**The linear regression equation and the graph of the obtained equation, R and R^2 values**
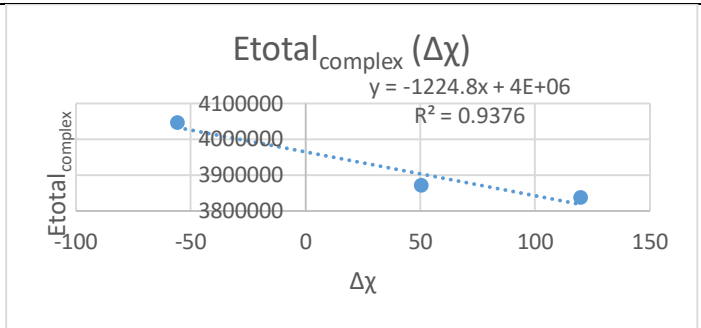 **Etotal$_{complex}$ (Δχ)** = - 1224.751 **Δχ** + 3964251.93 R = 0.96831697	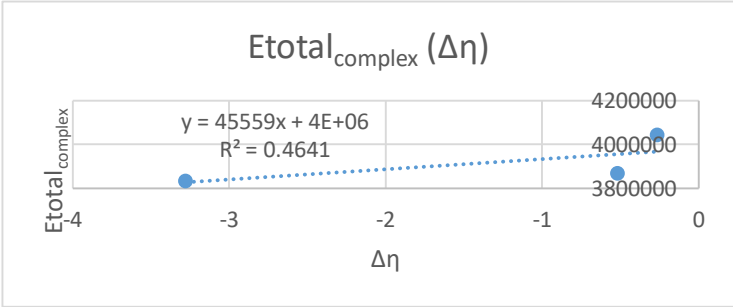 **Etotal$_{complex}$ (Δη)** = 45559.262 **Δη** + 3979340.32 R = 0.68124434
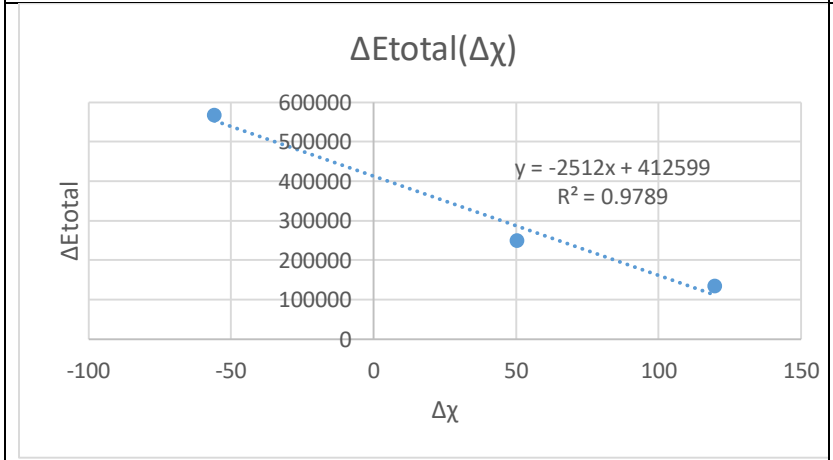 **ΔEtotal (Δχ)** = - 2511.99 **Δχ** + 412599.17 R = 0.98941168	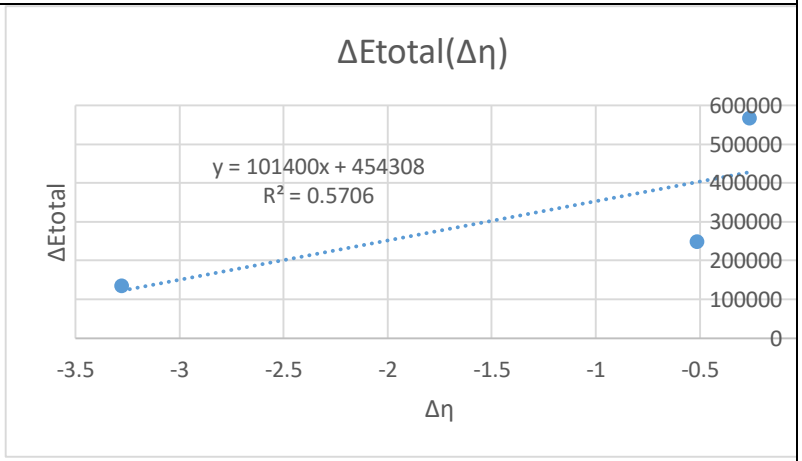 **ΔEtotalΔη)** = 101400.33**Δη** + 454307.68 R = 0.75536176

The linear regression equation and the graph of the obtained equation, R and R^2 values	The linear regression equation and the graph of the obtained equation, R and R^2 values
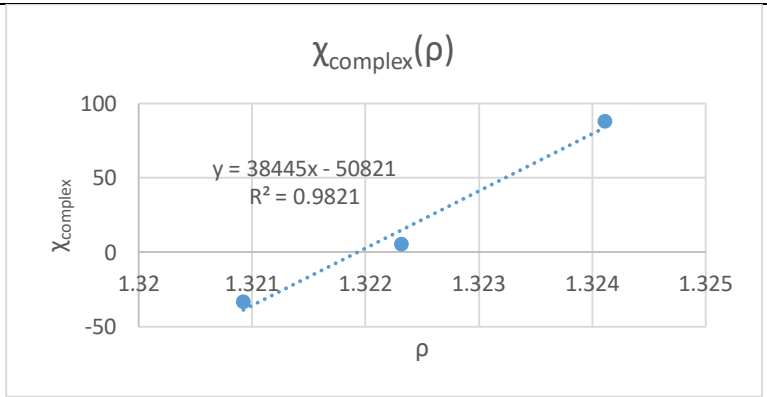 $\chi_{complex}(\rho)$ = 38444.59 ρ - 50820.985 2 R = 0.99101500	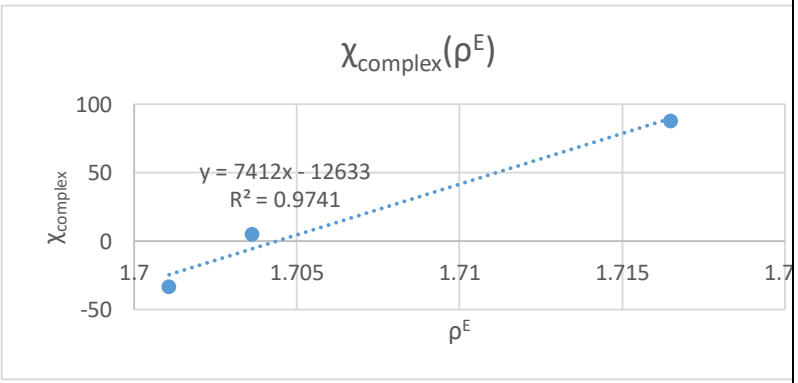 $\chi_{complex}(\rho^E)$ = 7411.976 ρ^E - 12632.6546 R = 0.98696893
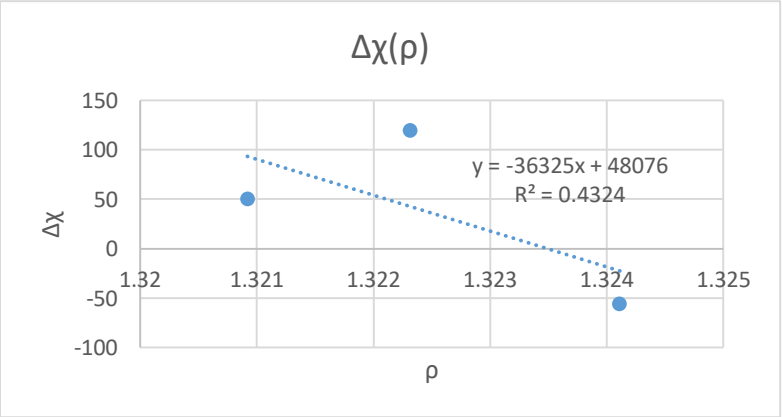 $\Delta\chi(\rho)$ = - 36325.22 ρ + 48076.217 R = 0.65753883	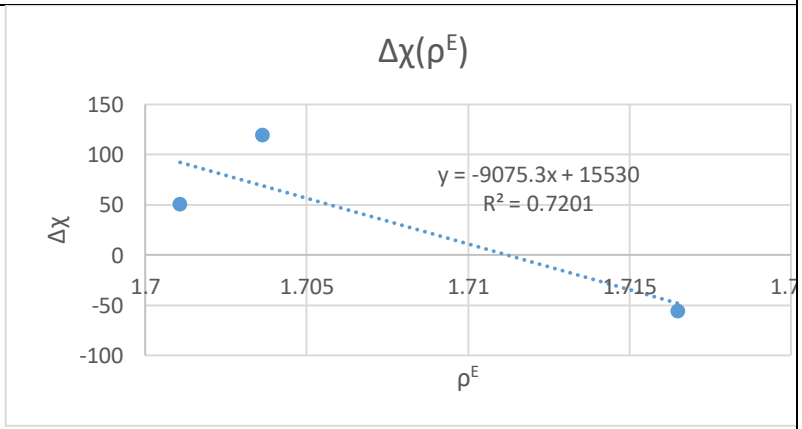 $\Delta\chi(\rho^E)$ = - 9075.282 ρ^E + 15529.99 R = 0.84858966

The linear regression equation and the graph of the obtained equation, R and R^2 values	**The linear regression equation and the graph of the obtained equation, R and R^2 values**
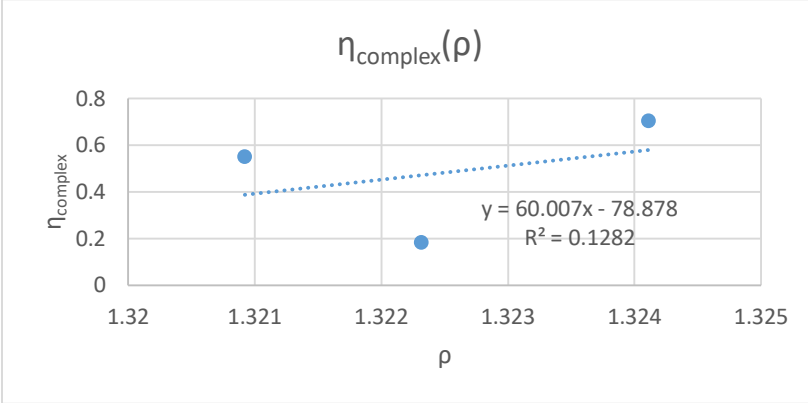 $\eta_{complex}(\rho)$ = 60.00727 ρ - 78.87809 R = 0.35800058	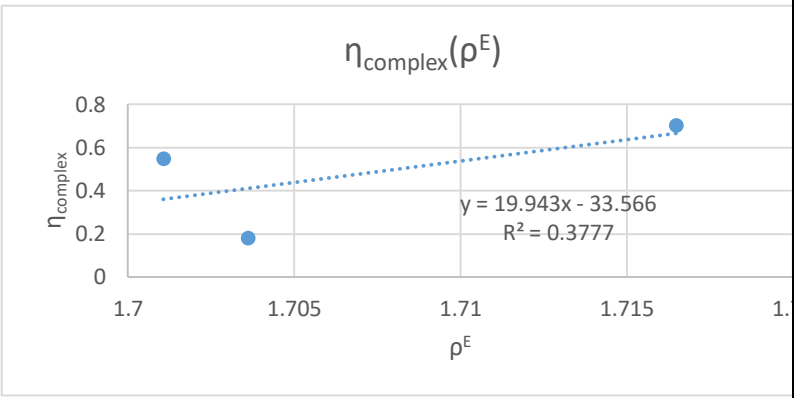 $\eta_{complex}(\rho^E)$ = 19.94323 ρ^E - 33.565784 R = 0.61461044
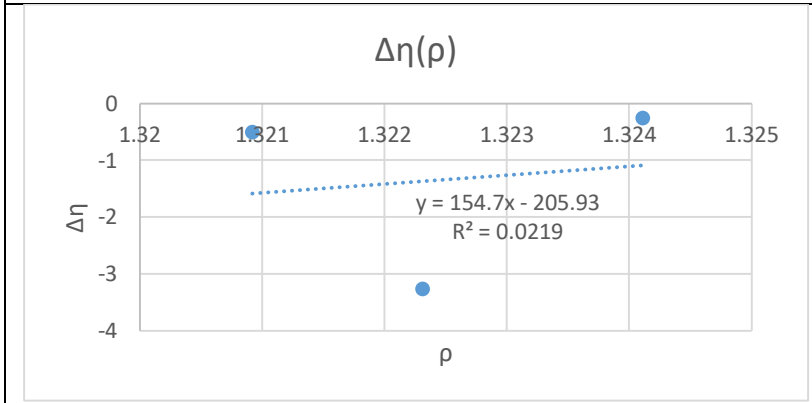 $\Delta\eta(\rho)$ = 154.698159 ρ- 205.93275 R = 0.14806136	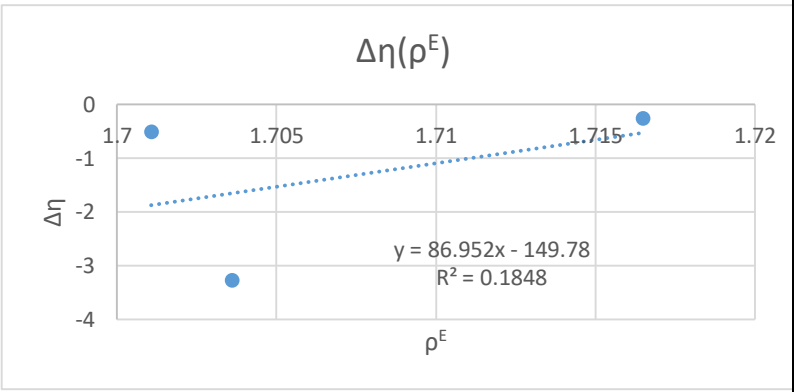 $\Delta\eta(\rho^E)$ = 86.9519 ρ^E - 149.784165 R = 0.42989285

The linear regression equation and the graph of the obtained equation, R and R^2 values	The linear regression equation and the graph of the obtained equation, R and R^2 values
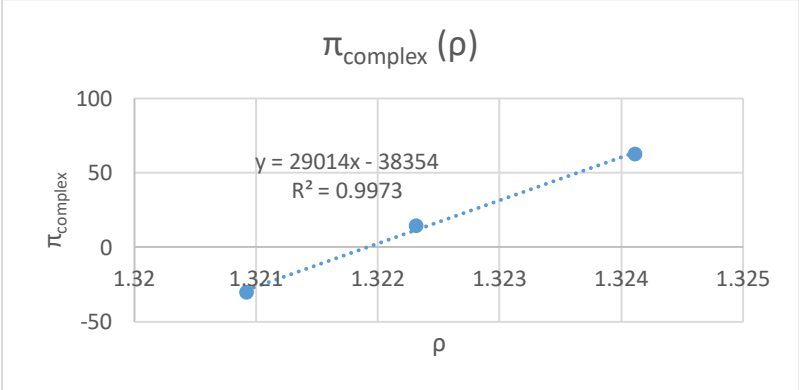 $\boldsymbol{\pi_{complex}(\rho)}$ = 29013.7989 **ρ** - 38353.706 R = 0.99862880	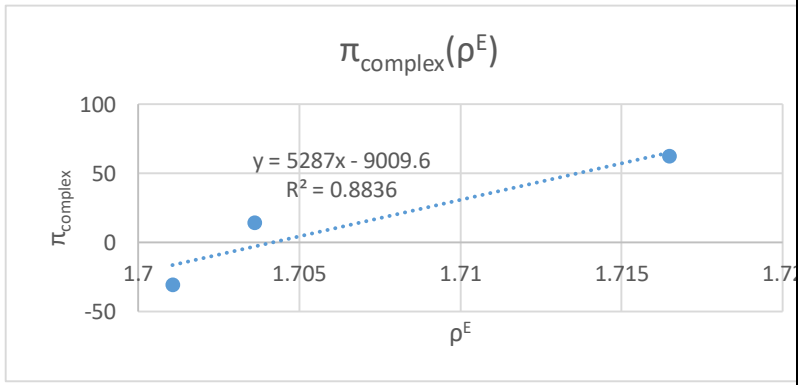 $\boldsymbol{\pi_{complex}(\rho^E)}$ = 5286.983 $\boldsymbol{\rho^E}$ - 9009.6319 R = 0.94000878
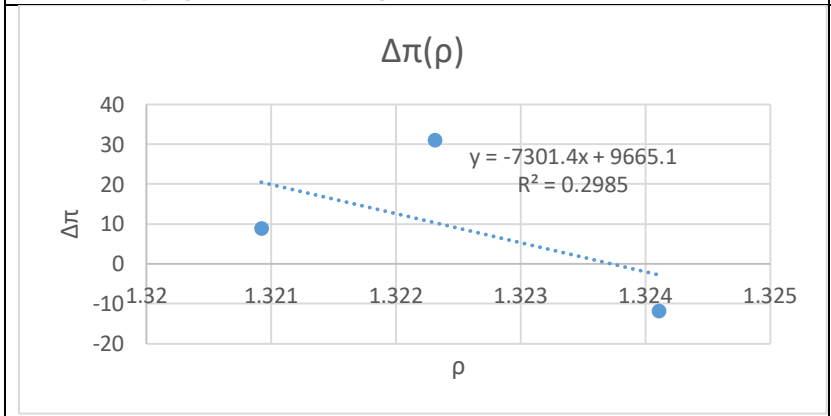 **Δπ(ρ)** = -7301.444 **ρ** + 9665.1284 R = 0.54637196	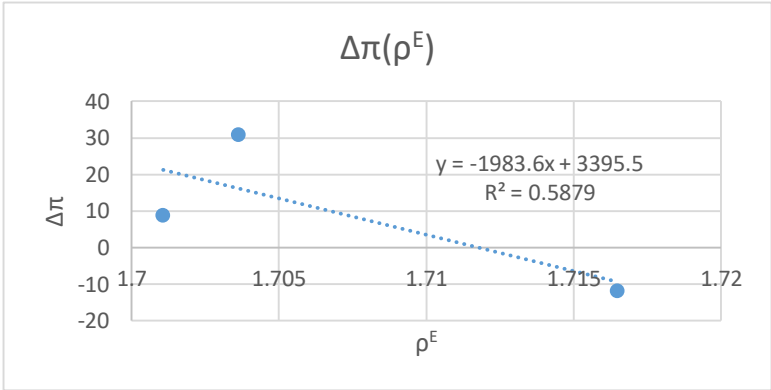 $\boldsymbol{\Delta\pi(\rho^E)}$ = - 1983.629 $\boldsymbol{\rho^E}$ + 3395.51075 R = 0.76676906

The linear regression equation and the graph of the obtained equation, R and R^2 values	**The linear regression equation and the graph of the obtained equation, R and R^2 values**
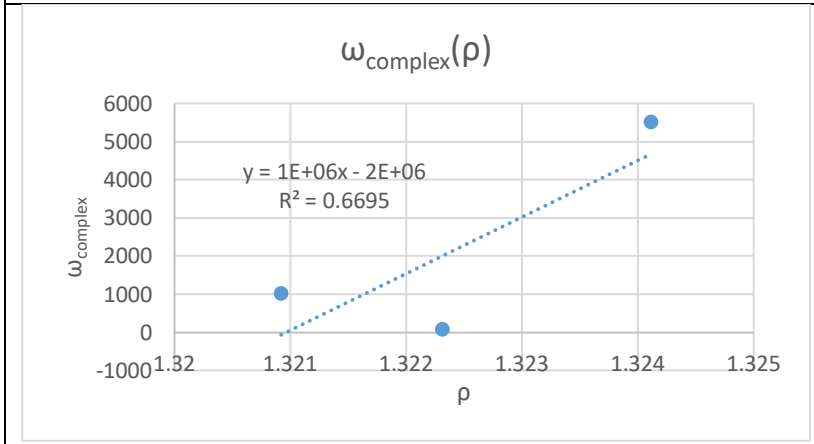 $\omega_{complex}(\rho)$ = 1486425.2 ρ - 1963519.926 R = 0.81822780	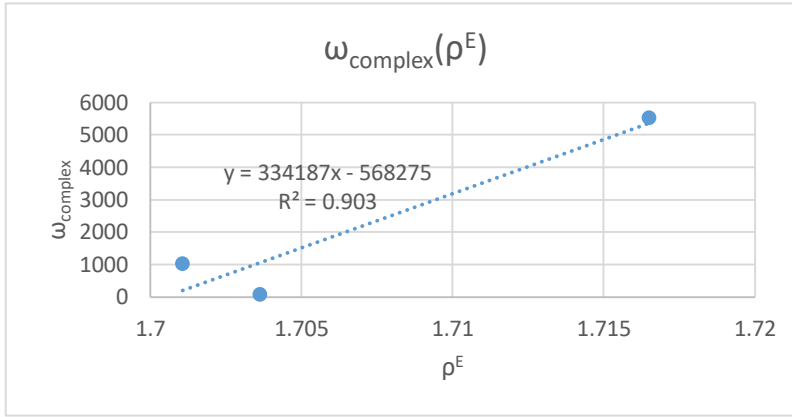 $\omega_{complex}(\rho^E)$ = 334186.87 ρ^E - 568275.01 R = 0.950265709
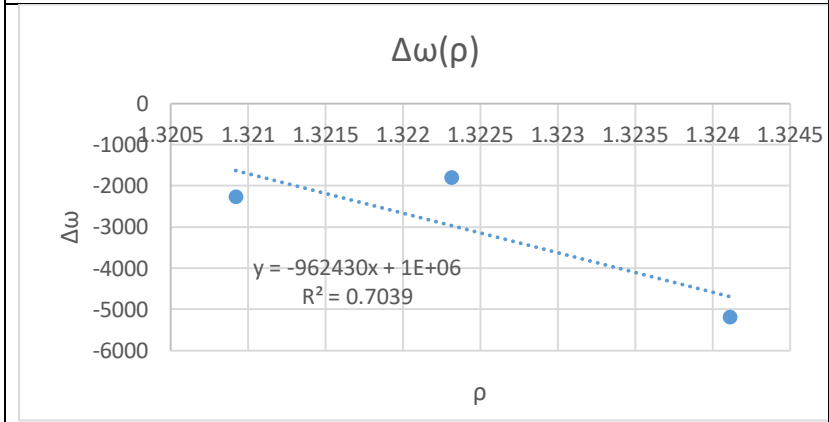 $\Delta\omega(\rho)$ = - 962430.08 ρ + 1269670.5 R = 0.83899019	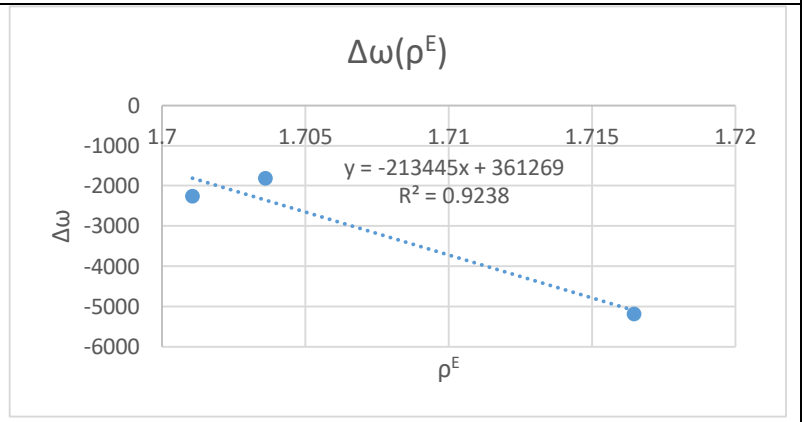 $\Delta\omega(\rho^E)$ = -213444.768 ρ^E + 361268.637 R = 0.96116448

Analyzing the results **from the chemical reactivity indices point of view** (see Table 3) it can be observed the following:

- $HOMO_{complex}$, $LUMO_{complex}$ have approximately the **same** degree of correlation R^2, with W respectively W_{exp}. Also the same degree of correlation have ΔHOMO, ΔLUMO with W respectively W_{exp}.
- For ΔHOMO the degree of correlation R^2 with W respectively, W_{exp} **increases** comparavetely with $HOMO_{complex}$. The same situation is also for ΔLUMO comparavetely with $LUMO_{complex}$:
  - R^2 : $HOMO_{complex} \approx LUMO_{complex}$ for W respectively W_{exp}
  - R^2 : ΔHOMO≈ ΔLUMO W for respectively W_{exp}
  - R^2 : ΔHOMO>$HOMO_{complex}$ for W respectively W_{exp}
  - R^2 : ΔLUMO> $LUMO_{complex}$ for W respectively W_{exp}.
- $Etotal_{complex}$ and ΔEtotal have approximately the **same** degree of correlation R^2 with W respectively W_{exp},
- In case of corelation between $Etotal_{complex}$ respectively ΔEtotal with **ρ** and $\boldsymbol{\rho^E}$, degree of correlation R^2 it is **better** in bouth cases for $\boldsymbol{\rho^E}$; when we compare $Etotal_{complex}$ with ΔEtotal degree of correlation R^2 it is **better** for $Etotal_{complex}$.
  - R^2 : $\boldsymbol{\rho^E > \rho}$ for. $Etotal_{complex}$ respectively ΔEtotal
  - R^2 : $Etotal_{complex}$ > ΔEtotal for $\boldsymbol{\rho^E}$ **si ρ**
- In case of corelation between $Etotal_{complex}$ respectively ΔEtotal with χ, Δχ, η, respectively Δη comparing the degree of correlation R^2 , it is observed that in the case of ΔEtotal correlation with Δχ the degree of correlation is extremely **good,** the entire comparation can be summarized as following:

R^2 **for** $\mathbf{Etotal_{complex}}$	$\chi_{complex} > \eta$	$\Delta\chi > \Delta\eta$	$\Delta\chi > \chi_{complex}$	$\Delta\eta > \eta_{complex}$
R^2 **for ΔEtotal**	$\eta > \chi_{complex}$	$\Delta\chi > \Delta\eta$	$\Delta\chi > \chi_{complex}$	$\Delta\eta > \eta_{complex}$
R^2 **for λ**	$Etotal_{complex}$ > ΔEtotal			
R^2 **for η**	ΔEtotal > $Etotal_{complex}$			
R^2 **for Δλ**	ΔEtotal > $Etotal_{complex}$			
R^2 **for Δη**	ΔEtotal > $Etotal_{complex}$			

Observing the degree of correlation $\mathbf{R^2}$ between **ρ** and $\boldsymbol{\rho^E}$ with the chemical reactivity indices, it reveals that in the case of the **stable** complex of molecular mashines type / rotaxane type as against of hierarchy *for chemical binding scenario* [10,47,48,61,62]

$$\chi \rightarrow \eta \rightarrow \pi \rightarrow \omega \qquad (9)$$

the hierarchy is as follows:

*The case of the **stable** complex of molecular mashines type / rotaxane type*	**π→**	**χ →**	**ω →**	**η**
R^2 for **ρ**	0.99725948	0.98211073	0.66949673	0.12816441
	χ →	**ω →**	**π→**	**η**
R^2 for $\boldsymbol{\rho^E}$	0.97410766	0.90300490	0.88361651	0.377745992

and for difference (Δ) of chemical reactivity indices, in the case of the **kinetic** complex of molecular mashines type / rotaxane type the hierarchy is as follows:

The case of the **kinetic** *complex of molecular mashines type / rotaxane type*	**Δω →**	**Δχ →**	**Δπ →**	**Δη**
R^2 for **ρ**	0.70390454	0.43235731	0.29852232	0.02192217
R^2 for $\boldsymbol{\rho}^{\mathbf{E}}$	0.92383715	0.72010442	0.58793478	0.18480786

From the topological point of view:

These molecular structures of calix[6]arenes complexes **1_4, 2_4, 3_4** with three kinds of guest molecules, 4,4'-bipyridinium dications, compounds **1, 2, 3,** and the host tris(N-phenylureido)-calix[6]arene - the calixarene wheel in rotaxane complex compound **4** have been herewith studied by ab-initio and topological methods. Energy calculations have been performed to gain more insight on the stabilizing effects coming by the host-guest interactions.

The simulation of the total potential energy indicates that the contribution which comes from the electrostatic polarization induced by the electric field of the guest gives a net stabilizing contribution whose values are listed in Table 4 below. Remarkably, the structural features of the present calix[6]arene derivatives confirm the validity of the "preorganization" principle early reported in literature that relies on appropriate variations of the molecular geometry of the ligands. The principle attributes an important role to the carbon/oxygen-chains of the host molecule which undertake specific the rearrangements to optimize the steric interface near the guest molecules. The preorganization mechanisms may vary, and may take place on different timescale, transforming the partial cone of the calix[6]arene to prepare it to form the new complexes **1_4, 2_4, 3_4.** Previous studies have determined that in these complexes the polar cage around the guest specie (molecules or even single cations) has normally the role of defining the position of the guest itself in respect to the barycentre of the interacting regions in the host, regions that quite often coincide with the volumes occupied by the nearest neighbor oxygens. In the present case in fact one may observe that the most significant structural deformations which preorganize the molecular structure of the polar cage to allow the formation of the complexes still consist in a geometrical distortion of the chains containing the oxygen atoms, see **Figure 5**. In these chains, topology attributes the highest the w_i=1006 (highest topo-reactivity) to the three terminal carbon atoms C37,C75,C114. Each chain starts form with an oxygen atom that functions like a sort of atomic hinge between the calixarene cone and the chain (**Figure 5**). *Vice versa, the carbon pairs C14/C16, C52/C54,* represent the most stable atoms in the core region of the topological structure of the ligand. The graphical representation of the complex **1_4** evidences large deformations in the structure of its ligand **4** that shows an almost flattened shape having lost the characteristics conic-shape. This flat structure, evidenced in **Figure 5**, is the proof of the massive preorganisational modifications undertaken by the calixarene to match with its molecular surface the shape of the guest molecule.

Figure 5: View of complex **1_4**. The hydrogen-deprived structure of the ligand is made by 117 non-hydrogen atoms with three dandling chains of sp^3 carbons ending with the highest topo-reactive atoms C37,C75,C114.The six atoms with minimum w_i are also represented. The structure of the ligand **4** shows a large distortion of the carbon chains, almost losing the characteristics calixarene cone-shape. The oxygen atoms at the basis of each chain work like atomic hinges and allowing the fluctuation of the chains.

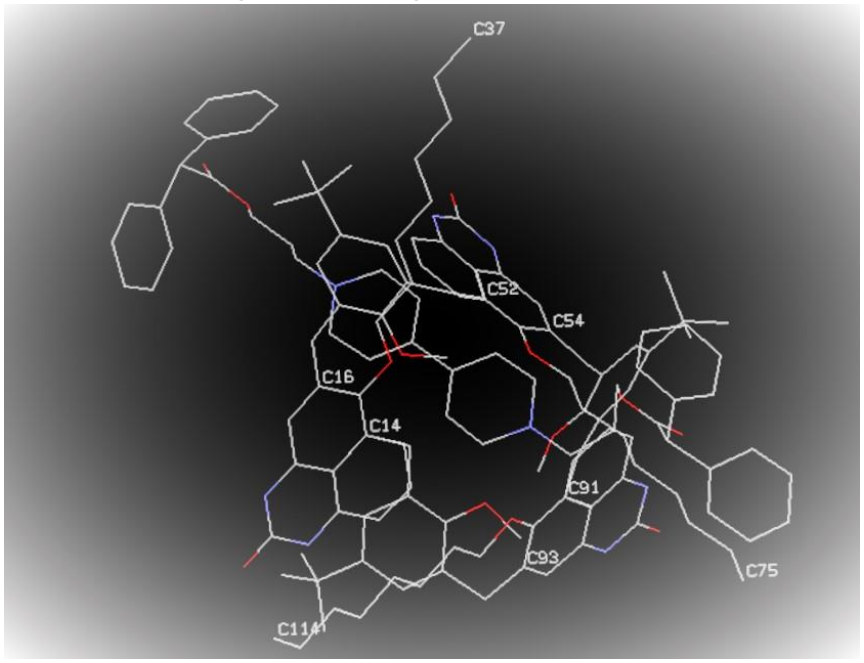

Regarding the relative stability of the three complexes, the simulations of the electronic properties performed in the present paper by quantum computational method are able to rank their relative electronic stability and the one of the preorganised ligand **1, 2, 3 or 4**. It is known from long time [68] that, by assuming the harmonic approximation for the entire crown ether chain, it is possible to estimate for each ligands the energy cost involved in the global deformations in the host-guest complexation process.

In agreement with this finding, the binding studies have shown that **1_4** is indeed the most efficient host-guest complex of the series. The energy values reported in Table 4 have been derived by the mean of original ab-initio computations and they show that ligand of the molecule **3_4** has the most preorganized structure, followed by **2_4** and **3_4**. The last derivative was found to be the least efficient of the remaining stereoisomers, thus indicating that the energy effects resulting by the oriented three carbon chains decrease the stability of the complex.

Another question that present studies pose it is why the ligands in the "partial cone and not those in the alternative conformations" prefer to bind the guest molecule in this series of calix[6]arenes complexes. To this extent, relevant non-bonding interactions are normally to be considered in order to simulate correctly the structural evolutions of the complex.

Topological modelling provides a fast and useful discrimination among these calixarene complexes **1_4, 2_4, 3_4** , the best candidate being the **2_4** system in which the total topological efficiency gets benefited by the complexation with the guest molecule **2,** the rotaxane **2_4,** Table 4 gives a clear overview of the current findings by listing the results of booth simulations, energetical and topological. The starred invariant indicates the **2_4,** as the one with the maximised topological efficiency.

Table 4: Energetic and topological parameters are reported for the host-guest complexes; in both cases the most stable systems are labelled by underscored values.

Rotaxane complex	**$Etotal_{precomplex}$ (kcal/mol)**	**$Etotal_{complex}$ (kcal/mol)**	**Complex topological efficiency (ρ/ρ*)**
1_4	3702346.613	3837167.691	1,0005
2_4	3621720.058	3870660.029	1
3_4	3477598.596	4045342.867	1,0012

The partial cone structure of the calix[6]arene derivatives seems to represent the best compromise between the stabilizing host-guest interaction and steric (repulsive) contributions. The stability of the **2_4** complex results moreover enhanced by considerations that come from the pure topology of that molecular system. In the present work we have found (see Table 4) the basal correlations between the stability/achievability of the calix[6]arene derivatives and the topological efficiency that represents a measure of a long-range extra symmetry aiming to homogenise the contribution to the Wiener index of every atoms to the one coming from the minimal vertices. The correlation between energetical parameters and topological efficiency has been also listed in the columns tabled and explained. Both these quantities have to be considered for predicting achievable calix[6]arene based structures.

The Wiener index is often used in drug screening because it correlates very well with the physico-chemical characteristics of the compounds (e.g. density, surface tension, van der Waals surface, etc.) but also to predict binding energy in a complex protein-ligand type [69,70]. Rotaxanes are also complexes but of molecular machines type, machines which execute a certain type of movement, movement which implies an exchange of energy between the parts of the complex.

As can be seen both the $Etotal_{complex}$ and the difference, ΔEtotal ($Etotal_{complex}$ - $Etotal_{precomplex}$) correlates very well with the Wiener index, *W*, which suggests a close connection between the total energy of the rotaxanic complex and the compaction of the complex (stabilization degree). The correlation with ΔEtotal being better suggests that at the transition from the precomplex stage to the complex stage, there is a stabilization between the two molecules of the complex due to the interactions and/or the intermolecular forces that are exerted between the two components of the rotaxanic complex, this being more compacted, more stable compared to the precomplex stage. This connection between the stability of the complex and its energy is also reinforced by the fact that $Etotal_{complex}$ and ΔEtotal correlate very well with the extreme topological efficiency index $\boldsymbol{\rho^E}$, which is also related to the stability of the complex [71]. The starred invariant indicates **2_4,** as the one with the maximized topological efficiency.

From the correlation between the energy ($Etotal_{complex}$, $\Delta Etotal$) and the chemical reactivity indices (χ, η, π, ω) respectively chemical reactivity indices and the topological indices ($\boldsymbol{\rho}$, $\boldsymbol{\rho}^{\mathbf{E}}$) it can be observed that $Etotal_{complex}$ and $\Delta Etotal$ of the rotaxanic molecular complexes with the difference of electronegativity ($\Delta\chi$) between the complex state and the precomplex state, i.e. with the tendency of the system to transfer electrons. On the second place is the correlation with $\chi_{complex}$, also related with the charge transfer in the rotaxanic complex and the alignment of the middy level of the HOMO-LUMO energy reactivity interval between the two components of rotaxane. It follows correlation with chemical hardness ($\eta_{complex}$), an index that with its maximization principle, expresses the charge transfer during a binding, a transfer that continues until the complex achieves its maximum stability by maximizing the HOMO-LUMO gap so that the next electronic transitions are prevente. For the transition from precomplex to complex stage, it is important the exchange of electrons between the components of rotaxane, respectively the delay of the moment of overcoming the HOMO-LUMO reactivity gap which prevents the final stabilization of rotaxane. This is also confirmed by the fact that $\eta_{complex}$ and $\Delta\eta$ correlate very weakly with $\boldsymbol{\rho}$, $\boldsymbol{\rho}^{\mathbf{E}}$ - topological efficiency indices (which indicate topological stability), the delayed maximization of the HOMO-LUMO gap allows continuous load transfer of electrons between the axle and the wheel of the rotaxane, fact that will would allow the execution of the rotation movement.

In the case of the correlations of chemical reactivity indices with $\boldsymbol{\rho}$, $\boldsymbol{\rho}^{\mathbf{E}}$ the best results were obtained for: $\chi_{complex}$, $\pi_{complex}$, $\Delta\omega$. Chemical power and electronegativity involves the transfer of electrons and the alignment of HOMO-LUMO median levels in the complex, these being involve in the topological stabilization of the rotaxanic complex; the difference in electrophilicity highlights the importance of breaking the energy barrier by the ondulatory charge transfer at the transition from the precomplex to the complex stage. This it also can be observe from the hierarchy for *chemical binding scenario* in the case of the **kinetic** complex ($\Delta\omega \rightarrow \Delta\chi \rightarrow \Delta\pi \rightarrow \Delta\eta$), hierarchy realized according to topological efficiency indices (topological stability of the rotaxanic complex). The stabilization of the **kinetic** complex is initiate by the electron ondulatory transfer that crosses the energy barrier between the wheel and the axle of rotaxane. This step is followed by the minimization of the difference of the median levels of the HOMO-LUMO energy reactivity interval between the axle and the wheel, followed by chemical power difference ($\Delta\pi$) – the transfer of the remaining electron. Final step in this hierarchy is the $\Delta\eta$, variation of chemical hardness, the extension of the HOMO-LUMO interval, the **kinetic** complex remains open for the charge transfer.

In the case of the **stable** complex of molecular machines type / rotaxane type the hierarchy for *chemical binding scenario* is different for the two considerated cases $\boldsymbol{\rho}$ **and** $\boldsymbol{\rho}^{\mathbf{E}}$**;** for $\boldsymbol{\rho}$ is $\pi \rightarrow \chi \rightarrow \omega \rightarrow \eta$, respectively for $\boldsymbol{\rho}^{\mathbf{E}}$ is $\chi \rightarrow \omega \rightarrow \pi \rightarrow \eta$. In both cases results a *chemical binding scenario* in which chemical reactivity indices are mixed (first generation: χ, η; second generation: π, ω). In the first case scenario begin with chemical power (π), namely the charge transfer without changing spin, followed by alignment of the middy level of the HOMO-LUMO energy reactivity interval between the two components of rotaxane. In the second case the stabilization of the complex is triggered by electronegativity (χ) and its principle of equalization of the median levels of the energy reactivity interval HOMO-LUMO, continues with one of the indices of the mixed reactivity: the electrophilicity (ω), namely the charge tunneling between the two components of the molecular machine. In both cases the hierarchy is ending with chemical hardness (η) maximizing the HOMO-LUMO energy gap. This particular behavior suggests that we are dealing with a system that remains open until the delayed maximization of

the HOMO-LUMO interval, fact that allows the continuous transfer of charge between the components of the rotaxane. This continuous transfer is also necessary in order to be able to perform a translational movement along the axle (or rotating around) of these complexes of molecular machines type, this motion implying a continuous charge transfer between the wheel and axle of the rotaxanic complex.

4. CONCLUSION

On calixare-based rotaxane complexes containing tris(N-phenylureido)-calix[6]arene as wheel and a 4,4'-bipyridinium dication's units as axle we applied topological-chemical reactivity studies (using electronegativity, chemical hardness, chemical power, electrophilicity indices and topological indices like Wiener indice). The results indicate that the most significant structural deformations, which preorganize the molecular structure of the polar cage to allow the formation of the complexes, consist in a geometrical distortion of the chains containing the oxygen atoms. Also it shows a massive preorganisational modifications undertaken by the calixarene to match with its molecular surface the shape of the guest molecule. The binding studies have revealed the most efficient host-guest complex of the serie. The starred invariant indicates the **2_4,** as the one with the maximized topological efficiency. The partial cone structure of the calix[6]arene derivatives seems to represent the best compromise between the stabilizing host-guest interaction and steric (repulsive) contributions. The stability of the **2_4** -complex results moreover enhanced by considerations that come from the pure topology of that molecular system.

From the very good correlation between energies and Wiener index, *W*, it can be concluded that at the transition from the precomplex stage to the complex stage, there is a stabilization between the two molecules of the complex due to the interactions and/or the intermolecular forces that are exerted between the two components of the rotaxanic complex, this being more compacted, more stable compared to the precomplex stage. From the correlation between the energy ($Etotal_{complex}$, $\Delta Etotal$) and the chemical reactivity we conclude that for the transition from precomplex to complex stage, it is important the exchange of electrons between the components of rotaxane, respectively the delay of the moment of overcoming the HOMO-LUMO reactivity gap which prevents the final stabilization of rotaxane.

From the correlations of chemical reactivity indices with $\boldsymbol{\rho}$, $\boldsymbol{\rho^E}$ we obtained the hierarchies for *chemical binding scenario* for the **kinetic** complex and the **stable** complex. It can be observed that all these hierarchies starts with the charge transfer without changing spin or charge tunneling followed by alignment of the middy levels of the HOMO-LUMO energy reactivity interval between the two components of rotaxane. All this hierarchies are ending with chemical hardness (η), namely the maximization the HOMO-LUMO energy gap. This behavior indicate that we are dealing with a system that remains open until the delayed maximization of the HOMO-LUMO interval, fact that allows the continuous transfer of charge between the components of the rotaxane. This delayed maximization may be necessary in order to be able to perform a translational movement along the axle (or rotating around) of these complexes of molecular machines type.

ACKNOWLEDGEMENTS

MVP acknowledges his contribution to this work within the Nucleus-Programme under the project PN-19-22-01-02 and its 2020 renewal as funded by the Romanian Ministry of Education and Research. Professors Margherita Venturi from University of Bologna (Italy) and Ioan Neda from Braunschweig Technical University (Germany) are hearty thanked for timely inspirational discussions on molecular machines and on calixarenes structures and properties, respectively.

REFERENCES

1. Desiraju, G. Chemistry beyond the molecule. *Nature* **2001,** *412*, 397–400.
2. Lehn, J.M. Supramolecular chemistry - scope and perspectives molecules, supermolecules and molecular devices. *Angew. Chem. Int. Edn*. **1988,** *27*, 89–112. 10.1002/anie.198800891
3. Stoddart, J.F. The chemistry of the mechanical bond. *Chem. Soc. Rev*. **2009,** *38*, 1802–1820.
4. Stoddart, J.F. Mechanically Interlocked Molecules (MIMs)—Molecular Shuttles, Switches, and Machines (Nobel Lecture) *Angew. Chem. Int. Ed.* **2017**, *56*, 11094 – 11125
5. Steed, J.W.; Atwood, J.L. *Supramolecular Chemistry* 2nd Ed, J. Wiley & Sons: Chichester, UK, 2009.
6. Ariga, K. Supermolecules, In *Biomaterials Nanoarchitectonics*, Ebara M. Eds. Publisher: William Andrew Publishing, NY, SUA, 2016, 25-40.
7. Balzani, V.; Credi, A.; Venturi, M. *Molecular Devices and Machines*; Wiley-VCH Verlag GmbH & Co. KGaA: Weinheim, Germany, 2008.
8. Teo, B.K.; Sun, X.H. From Top-Down to Bottom-Up to Hybrid Nanotechnologies: Road to Nanodevices *J. Clust. Sci.* **2006**, *17* (4), 529–540.
9. James, T.D. Specialty Grand Challenges in Supramolecular Chemistry. *Front Chem*. **2017**, *5*, 83. Published 2017 Oct 17. doi:10.3389/fchem.2017.00083
10. Dudaş, N.A.; Putz, M.V. Chemical reactivity driving switchable molecular machines. A case of Bipyridine -Calixarene rotaxane, *Fuller Nanotub Car N*, **2019,** *27:6*, 514-524, DOI: 10.1080/1536383X.2019.1612379
11. Neal, E.A.; Goldup, S.M. Chemical consequences of mechanical bonding in catenanes and rotaxanes: isomerism, modification, catalysis and molecular machines for synthesis. *Chem Commun (Camb)*. ***2014****; 50(40)*, 5128-5142.
12. Bruns, C.J.; Stoddart, J.F, *The Nature of the Mechanical Bond: From Molecules to Machines*, Wiley, New Jersey, SUA, 2016. p.1-90, 271-285.
13. Bruns, C.J.; Stoddart, J.F. Rotaxane-Based Molecular Muscles. *Acc. Chem. Res.*, **2014**, *47(7)*, 2186–2199.
14. Barin, G.; Forgan, R.S.; Stoddart, J.F. Mechanostereochemistry and the mechanical bond. *R. Soc. Lond. Proc. Ser. A Math. Phys. Eng. Sci.*, **2012,** *468*, 2849-2880.
15. McGonigal P.R. Multiply threaded rotaxanes, *Supramol. Chem.*, **2018,** *30(9)*, 782-794.
16. Dudaş, N.A.; Ori, O.; Putz, M.V. Challenging the HSAB principle on molecular machines' precursors. *Fuller Nanotub Car N* (**2021**) 29: 000-000 (in press); DOI: 10.1080/1536383X.2021.1877666.

17. Du, X.-S.; Wang, C.-Y.; Jia, Q.; Deng, R.; Tian, H.-S.; Zhang, H.-Y.; Meguellati, K.; Yang, Y.-W. Pillar[5]arene-based [1]rotaxane: high-yield synthesis, characterization and application in Knoevenagel reaction *Chem. Commun.* **2017**, *53*, 5326–5329.
18. Xu, K.; Nakazono, K.; Takata, T. Design of Rotaxane Catalyst for O-Acylative Asymmetric Desymmetrization of meso-1,2-Diol Utilizing the Cooperative Effect of the Components *Chem. Lett.* **2016**, *45*, 1274–1276.
19. Schalley, C.A.; Beizai, K; Vögtle, F On the Way to Rotaxane-Based Molecular Motors: Studies in Molecular Mobility and Topological Chirality. *Acc. Chem. Res.* **2001,** *34(6)*, 465–476
20. Sauvage, J.P. Transition Metal-Containing Rotaxanes and Catenanes in Motion: Toward Molecular Machines and Motors *Acc. Chem. Res.*, **1998**, *31(10)*, 611–619.
21. Xue, M.; Yang, Y.; Chi, X.; Yan, X.; Huang, F. Development of Pseudorotaxanes and Rotaxanes: From Synthesis to Stimuli-Responsive Motions to Applications *Chem. Rev.* **2015**, *115*, 7398–7501.
22. Venturi, M.; Iorga, M. I.; Putz, M.V. Molecular Devices and Machines: Hybrid Organic-Inorganic Structures *Current Organic Chemistry*, **2017**, *21*, 2731-2759
23. Arduini, A.; Bussolati, R.; Credi, A.; Pochini, A.; Secchi, A.; Silvi, S.; Venturi, M. Rotaxanes with a calix [6] arene wheel and axles of different length. Synthesis, characterization, and photophysical and electrochemical properties. *Tetrahedron*. **2008**; *64(36)*, 8279-8286.
24. Balzani, V.; Credi, A.; Venturi, M. *Molecular Devices and Machines*. *Concepts and Perspectives for the Nanoworld*; Wiley-VCH: Weinheim, Germany, 2008.
25. Monk, P.M.S *The Viologens - Physicochemical Properties Synthesis and application of the salts of 4,4'-Bipyridine*; Wiley: Chichester, UK, 1998.
26. Ballardini, R.; Credi, A.; Gandolfi, M. T.; Giansante, C.; Marconi, G.; Silvi, S.; Venturi, M. Photophysical, photochemical and electrochemical properties of a series of aromatic electron acceptors based on N-heterocycles. *Inorg. Chim. Acta*. **2007**, *360*(3), 1072-1082.
27. Orlandini, G.; Ragazzon, G.; Zanichelli, V.; Degli Esposti, L.; Baroncini, M.; Silvi, S.; Venturi, M.; Credi, A.; Secchi, A.; Arduini, A. Plugging a Bipyridinium Axle into Multichromophoric Calix[6]arene Wheels Bearing Naphthyl Units at Different Rims. *ChemistryOpen*. **2017**; *6(1)*, 64-72.
28. Guérineau, V.; Rollet, M.; Viel, S.; Lepoittevin, B.; Costa, L.; Saint-Aguet, P.; Laurent, R.; Roger, P.; Gigmes, D.; Martini, C.; Huc, V. The synthesis and characterization of giant Calixarenes *Nature Communications* **2019,** *10*, Article number: 113, https://doi.org/10.1038/s41467-018-07751-4
29. Arora, V.; Chawla, H.; Singh, S.P. Calixarenes as Sensor Materials for Recognition and Separation of Metal Ions.*ARKIVOC* **2007**, *ii*, 172-200.
30. Cragg, P.J. *Supramolecular Chemistry: From Biological Inspiration to Biomedical Applications*, **2010**, Springer, USA; p.1-48
31. Gutsche, C D. -Calixarenes: An Introduction, Ed. 2, In *Monographs in Supramolecular Chemistry*, The Royal Society of Chemistry, UK, 2008
32. Agrawal, Y.K., Pancholi, J., Vyas, J.M. Design and synthesis of calixarene. *J SCI IND RES INDIA* **2009,** *68(9)*, 745-768
33. Yang, F.; Guo, H.; Vicens, J. Mini-review: Calixarene liquid crystals. *J. Incl. Phenom. Macrocycl. Chem*. **2014**, *80*, 177–186
34. Da Silva, E.; Ficheux, D.; Coleman, A.W. Anti-thrombotic activity of water-soluble calix[n]arenes. *J. Incl. Phenom. Macrocycl. Chem*. **2005**, *52*, 201–206.
35. Arduini, A.; Ferdani, R.; Pochini, A.; Secchi, A.; Ugozzoli, F. Calix[6]arene as a Wheel for Rotaxane Synthesis *Angew. Chemie, Int. Ed.* **2000**, *39*(19), 3453–3456.

36. Arduini, A.; Calzavacca, F.; Pochini, A.; Secchi, A. Unidirectional Threading of Triphenylureidocalix[6]arene-Based Wheels: Oriented Pseudorotaxane Synthesis *Chem. - A Eur. J.* **2003**, *9* (3), 793–799.
37. Arduini, A.; Ciesa, F.; Fragassi, M.; Pochini, A.; Secchi, A. Selective Synthesis of Two Constitutionally Isomeric Oriented Calix[6]arene-Based Rotaxanes *Angew. Chem., Int. Ed.* **2005**, *44*, 278–281.
38. Ugozzoli, F.; Massera, C.; Arduini, A.; Pochini, A.; Secchi, A. Calix [6] arene-based pseudorotaxanes: a solid state structural investigation. *CrystEngComm*, **2004,** *6(39)*, 227-232.
39. Arduini, A.; Bussolati, R.; Credi, A.; Secchi, A.; Silvi, S.; Semeraro, M.; Venturi, M. Toward Directionally Controlled Molecular Motions and Kinetic Intra- and Intermolecular Self-Sorting: Threading Processes of Nonsymmetric Wheel and Axle Components *J.Am. Chem. Soc.* **2013**, *135* (26), 9924–9930.
40. Zanichelli, V., Ragazzon, G., Orlandini, G., Venturi, M., Credi, A., Silvi, S., Arduini, A., & Secchi, A. (**2017**). Efficient active-template synthesis of calix[6]arene-based oriented pseudorotaxanes and rotaxanes. *Organic & biomolecular chemistry*, *15 32*, 6753-6763 .
41. Zanichelli, V.; Bazzoni, M.; Arduini, A.; Franchi, P.; Lucarini, M.; Ragazzon, G.; Secchi, A.; Silvi, S. Redox-Switchable Calix[6]arene-Based Isomeric Rotaxanes *Chem. Eur.J* .**2018**, *24*,12370–12382
42. Zanichelli, V.; Dallacasagrande, L.; Arduini, A.; Secchi, A.; Ragazzon, G.; Silvi, S.; Credi, A. Electrochemically Triggered Co-Conformational Switching in a [2]catenane Comprising a Non-Symmetric Calix[6]arene Wheel and a Two-Station Oriented Macrocycle. *Molecules* **2018**, *23*, 1156.
43. Bazzoni, M.; Zanichelli, V.; Casimiro, L.; Massera, C.; Credi, A.; Secchi, A.; Silvi, S.; Arduini, A. New Geometries for Calix[6]arene-Based Rotaxanes, *Eur. J. Org. Chem.*, **2019**, *21*, 3513-3524.
44. Orlandini, G.; Casimiro, L.; Bazzoni, M.; Cogliati, B.; Credi, A.; Lucarini, M.; Silvi, S.; Arduini, A.; Secchi, A. Synthesis and properties of a redox-switchable calix[6]arene-based molecular lasso, *Org. Chem. Front.*, **2020**, doi:10.1039/C9QO01379B
45. Zanichelli, V.; Dallacasagrande, L.; Arduini, A.; Secchi, A.; Ragazzon, G.; Silvi, S.; Credi, A. Electrochemically Triggered Co-Conformational Switching in a [2]catenane Comprising a Non-Symmetric Calix[6]arene Wheel and a Two-Station Oriented Macrocycle. *Molecules*, **2018**, *23*, 1156.
46. Gaeta,C.; Talotta,C.; Neri,P. Calix[6]arene-based atropoisomeric pseudo[2]rotaxanes *Beilstein J. Org. Chem.* **2018,** *14*, 2112–2124. doi:10.3762/bjoc.14.186
47. Putz, M.V.; Dudaş, N.A**.** Variational principles for mechanistic quantitative structure–activity relationship (QSAR) studies: application on uracil derivatives' anti-HIV action. *Struct. Chem.*, **2013**, *24*, 1873.
48. Putz, M.V.; Dudaş, N.A. Determining Chemical Reactivity Driving Biological Activity from SMILES Transformations: The Bonding Mechanism of Anti-HIV Pyrimidines. *Molecules* **2013**, *18*, 9061-9116.
49. Putz, M.V.; Ori, O.; Cataldo, F.; Putz, A.M. Parabolic reactivity <<coloring>> molecular topology. Application on carcinogenic PAHs. *Curr. Org. Chem.* **2013**, *17*, 2816–2830.
50. Putz, M.V.; Putz, A.M. DFT chemical reactivity driven by biological activity: applications for the toxicological fate of chlorinated PAHs. *Struct Bond* **2013,** *150*, 181–232

51. Iczkowski R.P.; Margrave, J.L. Electronegativity. *J Am Chem Soc* **1961,** *83*, 3547–3551
52. Parr, R.G.; Donnelly, R.A.; Levy, M.; Palke, W.E.; Electronegativity: the density functional viewpoint. *J Chem Phys* **1978**, *68*:3801–3808
53. Putz, M.V. Systematic formulation for electronegativity and hardness and their atomic scales within density functional softness theory. *Int J Quantum Chem* **2006,** *106*, 361–389.
54. Putz, M.V.Electronegativity: quantum observable. *Int J Quantum Chem* **2009,** *109*, 733–738
55. Parr, R.G.; Yang, W. *Density-Functional Theory Of Atoms And Molecules*; Oxford University Press: New York, NY, USA, 1989.
56. Putz, M.V.; Russo, N.; Sicilia, E. About the Mulliken electronegativity in DFT. *Theor Chem Acc* **2005,** *114*, 38–45
57. Parr, R.G.; Pearson, R.G. Absolute hardness: companion parameter to absolute electronegativity. *J. Am. Chem. Soc.*, **1983**, *105 (26)*, 7512–7516
58. Pearson, R.G. Absolute electronegativity and absolute hardness of Lewis acids and bases. *J Am Chem Soc* **1985,** *107*, 6801–6806
59. Pearson, R.G. *Chemical hardness*. Wiley-VCH, Weinheim, Germany, 1997.
60. Putz, M.V. *Absolute and chemical electronegativity and hardness*. Nova Science Publishers Inc., New York, USA, 2008
61. Pearson, R.G. *Hard and soft acids and bases*. Dowden, Hutchinson & Ross, Stroudsberg, Germany, 1973
62. Pearson, R.G. Hard and soft acids and bases—the evolution of a chemical concept. *Coord Chem Rev* **1990,** *100*, 403–425
63. a)Putz, M.V.; Tudoran, M.A. Bondonic effects on the topo-reactivity of PAHs. *Int J Chem Model* **2014**, *6(2–3)*, 311–346. b) Putz, M.V.; Ori, O.; De Corato, M.; Putz, A.M.; Benedek, G.; Cataldo, F.; Graovac, A. Introducing "Colored" Molecular Topology by Reactivity Indices of Electronegativity and Chemical Hardness. In: *Topological Modelling of Nanostructures and Extended Systems. Carbon Materials: Chemistry and Physics*, Ashrafi A.; Cataldo F.; Iranmanesh A.; Ori O. Eds., Volume 7, Publisher: Springer, Dordrecht, NL, 2013, pp. 265-287.
64. Ori, O.; Putz, M.V. Topological evolution of the 5|8|5 defect in *graphene New Front. Chem.*,**2018**, *27*(2), 105-113
65. Wiener, H. Structural determination of paraffin boiling points *J. Am. Chem. Soc.*, **1947,** *1(69*), 17–20
66. Devillers, J.; Balaban, A.T. (Eds.) Topological Indices and Related Descriptors in QSAR and QSPR, Publisher: Gordon & Breach, Amsterdam, Holland, 1999.
67. Hypercube, Inc. (**2002**) HyperChem 7.01 [Program Package]; Hypercube, Inc.: Gainesville, FL, USA.
68. Ugozzoli, F.; Ori, O.; Casnati, A.; Pochini, A.; Ungaro, R.; Reinhoudt D.N. Evidence for cation-π interactions in calixcrown·KPic complexes from X-ray crystal structure analysis and energy calculations, *Supramolecular Chemistry*, **1995,** *5:2*, 179-184, DOI: 10.1080/10610279508029492
69. Estrada, E.; Patlewicz, G.; Uriarte, E. From molecular graphs to drugs. A review on the use of topological indices in drug design and discovery. *Indian J. Chem.*, **2003,** *42*, 1315-1329

70. Rouvray, D.H. The rich legacy of half century of the Wiener index, in *Topology in Chemistry: Discrete Mathematics of Molecules*, Rouvray, D.H.; King, R.B.; Eds.; Publisher: Horwoord, Chichester, UK; 2002, pp. 16-37
71. Koorepazan-Moftakhar, F.; R Ashrafi, A.; Ori, O.; Putz, M.V. Topological invariants of nanocones and fullerenes. *Curr. Org. Chem.*, **2015,** *19(3)*, 240-248.